SDSS'Rio 2010 STABILITY AND DUCTILITY OF STEEL STRUCTURES
E. Batista, P. Vellasco, L. de Lima (Eds.)
Rio de Janeiro, Brazil, September 8 - 10, 2010

LATERAL BUCKLING OF CONTINUOUS STEEL BEAMS WITH HINGES

Peter Osterrieder*, Stefan Richter*, Matthias Friedrich**

* Faculty of Architecture, Civil Engineering and Urban Planning,
Brandenburg Technical University BTU Cottbus, D-03044 Cottbus, FRG,
e-mails: lsud@statik.tu-cottbus.de
** Friedrich+Lochner GmbH, D-01067 Dresden, FRG

Keywords: Lateral torsional buckling, local hinges, first-yield design, warping torsion of open thin-walled members.

Abstract. *Continuous steel beams used for girders, purlins, crane girders, etc. are subjected to lateral torsion buckling. In many cases construction joints of those beams are carried out as moment hinges rather than as rigid connections. The study is concerned with the effect of these hinges on the lateral stability behaviour and their effect on the design. Based on a numerical approach critical lateral buckling loads are calculated for different hinge locations and moment distributions. Finally load capacities obtained from equivalent slenderness approach are compared to those from first-yield criterion with internal forces from theory 2nd order analysis.*

1 INTRODUCTION

Figure 1 shows common type of construction joints for continuous I-beams which will be assembled on the construction site. These joints are able to transfer shear forces but only small fractions of the bending, torsion and warping moments associated with 3-dimensional loading and nonuniform torsion. Therefore in the structural analysis it is assumed for the hinge that lateral displacements v and w are compatible and

$$M_y = M_z = M_x = M_\omega = 0 \tag{1}$$

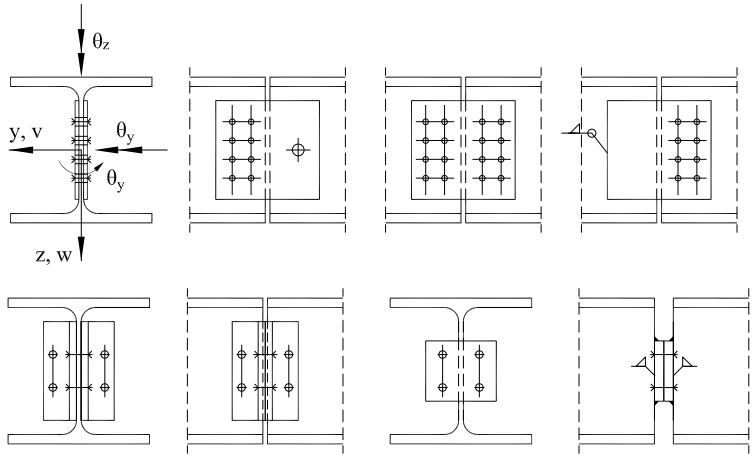

Figure 1: Examples of common construction joints for continuous beams

While moment hinges may be easily considered in any commercial computer program for in-plane stress analysis the allowance of local static boundary conditions in the eigenvalue calculation required for lateral buckling design is rather unusual. To account for local boundary conditions within a displacement based finite element formulation basically two alternatives are available. Applying as usual static condensation to local element stiffness matrix leads to coupled elastic and geometric element matrices which are not suitable for numerical eigenvalue solution applying vector iteration. Introducing instead double nodes and incorporating coupling conditions during assembly of the system stiffness results in uncoupled elastic and geometric system stiffness matrices. The latter approach has been applied to a FE-program for nonlinear analysis of 3-D beams with open thin-walled cross sections [1]. Bifurcation loads from this numerical approach are applied to check for lateral buckling according to Eurocode 3 [2, paragraph 6.3.2.2]. Design loads from this approach are compared to ultimate loads obtained by an elastic theory 2nd order analysis considering geometric out-of-plane imperfections according to [2, paragraph 5.3.2].

2 NUMERICAL EIGENVALUE APPROACH

As described above the eigenvalue problem of a continuous beam with a local hinge has been solved within a geometric nonlinear formulation by introduction of double nodes with subsequent coupling of dofs during the assembling process of elastic and geometric system stiffness matrices. Two procedures are available for the numerical solution of the general eigenvalue problem $\det(\mathbf{A}-\lambda\mathbf{B}) = 0$. First a rather simple algorithm based on a modified inverse iteration with random generated starting vectors and automatic shifting is started. If no convergence is reached subspace iteration with QZ-Algorithm is initiated. To verify the procedure bifurcation loads for beams with moment hinge at midspan (fig. 2) have been compared with closed-form and numerical solutions.

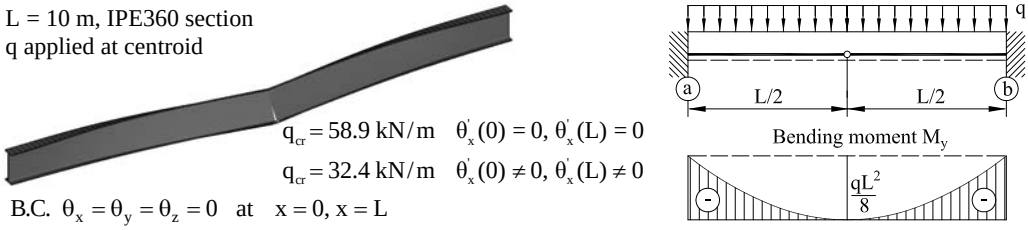

Figure 2: Lateral torsional buckling of beam with hinge

Critical loads for a cantilever beams which is equivalent to the structural system in figure 2 with a span of 5m are calculated from analytical equations in [3, eqns.(9.14), (9.17)] as $q_{cr} = 57{,}2$ kN ($\theta_x' = 0$ at both ends) and $q_{cr} = 27.9$ kN ($\theta_x' \neq 0$ at both ends) with θ_x' as the warping displacement. Numerical results for the cantilever beam obtained from [1] are identical to those given for the entire beam with the hinge in figure 2.

Specific attention is required, when the joint design in addition cannot transfer shear forces in y-direction at all or only with considerable web deflections. In this case the left and the right side of the beam is essentially uncoupled and so lateral buckling behaviour of the two substructures.

Figure 3: Lateral torsional buckling mode of mono symmetric beam with moment hinge

If the cross section is not doubly symmetric as shown in figure 3, displacements v und w in the direction of the major y- and z-axes are related to the shear centre of the cross section.

3 CRTITICAL LOADS FOR CONTINUOUS BEAMS WITH HINGES

3.1 Structural idealization

To check any continuous beam as shown in figure 4 for lateral torsional buckling applying equivalent slenderness procedure the associated lowest eigenvalue q_{cr} for the entire structural system is required.

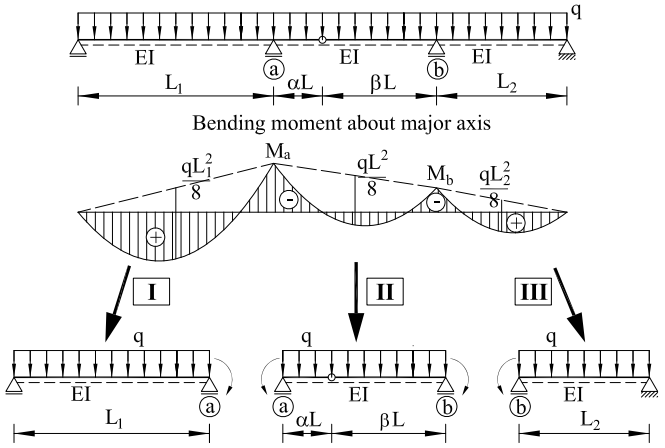

Figure 4: Continuous beam with moment hinge in midspan

Most common q_{cr} is calculated alternatively in engineering practice for a virtually cut out single span beam only with appropriate geometric and static boundary conditions at the respective supports. The lateral torsional stability is governed by weakest – the most slender – beam. The interaction between the single spans depends not only on the major axis bending moments but especially on the boundary conditions for out-of-plane bending (v, θ_z) and torsion (θ_x, θ_x'). While in most real structures lateral deformations v and torsional rotations θ_x at the supports will be restrained, boundary conditions for θ_z and θ_x' depend strongly on the out-of-plane bending and torsional stiffness of the adjacent spans. To illustrate the sensitivity of the buckling load q_{cr} with respect to the b.c. critical loads are calculated for the three single spans in fig. 4 with and without warping restraint at the ends and related to the critical value q_{cr} = 24,94 kN/m for the entire system. Results in table 1 are for $L_1 = L_2$ = 8m, L = 10m, α = 0.3 and IPE330 section. To avoid kinematics in the eigenvalue analyses for span II the rotation at the right end about the major y-axis is completely restrained.

For critical loads in row 2 it is assumed that the rotation θ_z about the weak z-axis is completely restrained for all beams at the intermediate supports. Results in row 3 are calculated for unrestrained rotations θ_z in a for the left beam, in b for the right beam and the rotation spring stiffness

$$k_{\theta z} = 3\frac{EI_z}{L_1} = 620{,}6\left[\frac{kNm}{rad}\right] \tag{2}$$

at both supports of the beam with hinge. From the results in table 1 it is obvious, that buckling of the middle span governs the stability problem and further that the middle span is elastically restrained against out-of-plane bending and warping by both outer spans. More general it can be concluded that for most practical problems of continuous beams the span containing the hinge will be relevant for stability

design. Thus the critical load may be approximated considering only the span with the moment hinge. Fully warping restraint at both supports leads to the upper bound and free warping to the lower bound for the critical eigenvalue.

Table 1: Critical loads $\overline{q}_{cr}$

1	span I		span II		span III	
	$\theta'_{x,a}=0$	$\theta'_{x,a}\neq 0$	$\theta'_{x,a}=0$ $\theta'_{x,b}=0$	$\theta'_{x,a}\neq 0$ $\theta'_{x,b}\neq 0$	$\theta'_{x,b}=0$	$\theta'_{x,b}\neq 0$
2	1.58	1.26	1.22	0.95	1.31	1.11
3	1.55	1.26	1.20	0.95	1.19	1.05

From the smallest critical load the critical moment and the dimensionless lateral torsional buckling slenderness

$$\bar{\lambda}_{LT}=\sqrt{\frac{W_y f_y}{M_{cr}}} \tag{3}$$

has to be evaluated for the subsequent design check.

3.2 Critical Loads for single span beams with a moment hinge

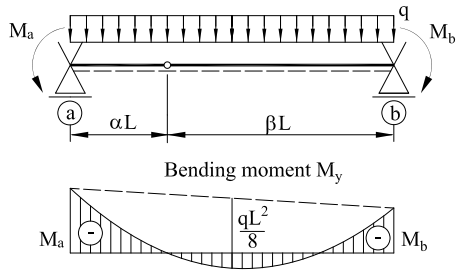

Figure 5: Bending moment distribution for single span beam with hinge

For a single span beam with a moment hinge as specified in eqn. (1) at distance αL from the left end (fig. 5) the moment M_b at the right end depends further on the moment M_a and the uniformly distributed load q

$$M_b=\beta\left(\frac{qL^2}{2}-\frac{Ma}{\alpha}\right) \tag{4}$$

As long as the hinge is close to the centre of the span the left and the right segments will interact in lateral torsional buckling depending on the bending moment distribution. When the hinge gets closer to the right or left bearing, the shorter beam segment will support the longer segment in the out-of-plane behaviour. For a hinge very close to one of the bearings the out-of-plane boundary conditions at the hinge for the remaining longer segment may be approximated as

$$v=0 \quad \theta_z\neq 0 \quad \theta_x\neq 0 \quad \theta'_x\neq 0 \tag{5}$$

Figure 6 shows a comparison of critical loads and associated eigenmodes for a beam with uniformly distributed load q, a hinge at α = 0.3 and equivalent bending moment distributions about major y-axis in

both systems. The total buckling mode is governed by the weaker beam segment and differs from the partial mode only slightly with an increase in the critical load for the partial system of 11%.

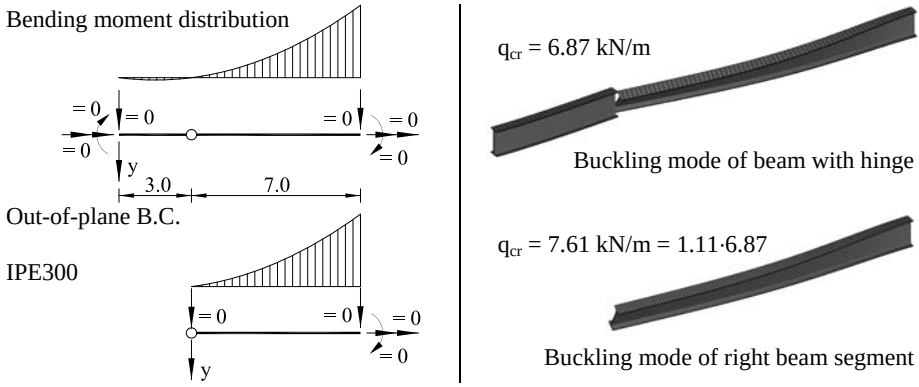

Figure 6: Buckling modes and buckling loads for total and partial structure

Results in table 2 for a beam with a total span of 10 m, IPE300 section, varying hinge location α, out-of-plane b.c. as shown in fig. 6 and bending moment $M_a = 0$ confirm this observation more generally.

Table 2: Comparison of critical loads

A	q_{cr} [kN/m] total beam	q_{cr} [kN/m] right segment
0.5	8.30	13.09
0.4	7.42	9.67
0.3	6.87	7.61
0.2	6.10	6.25
0.1	5.29	5.30

In figures 7 to 9 the dimensionless critical buckling loads

$$\bar{q}_{cr} = \frac{q_{cr} L^3}{\sqrt{EI_z GI_t}} \tag{6}$$

for beams with hinge b.c. given in eqn. (1) and $\theta_z = 0$ at both supports are plotted over the stiffness coefficient

$$k = \frac{\pi}{L}\sqrt{\frac{EI_\omega}{GI_t}} \tag{7}$$

In [3] and similar in [4] it has been shown, that critical loads presented in this dimensionless form are applicable to almost any beam with hot-rolled doubly symmetric I-section. From figs. 7b to 9b it follows that for beams restrained against warping at the ends the relation between the dimensionless stiffness and the dimensionless critical load is almost linear. For beams with free warping b.c. at both ends the relation is found to be highly nonlinear with almost asymptotic behaviour for increasing stiffness.

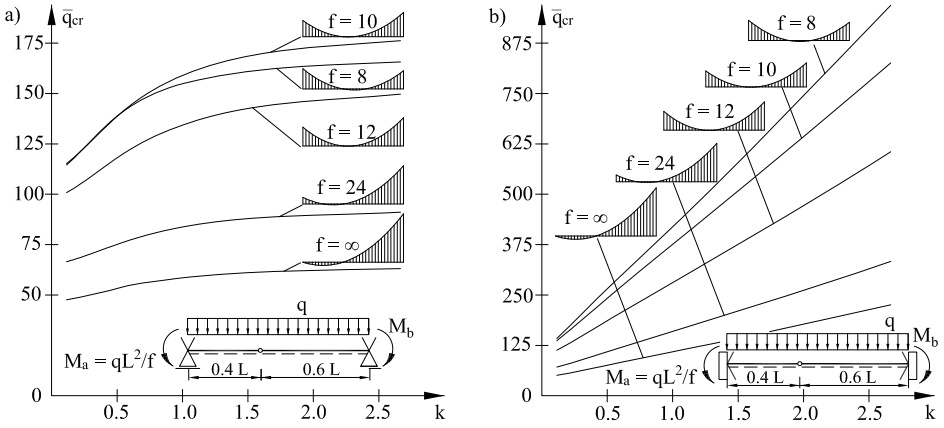

Figure 7: Critical loads for beam with hinge at α = 0.4

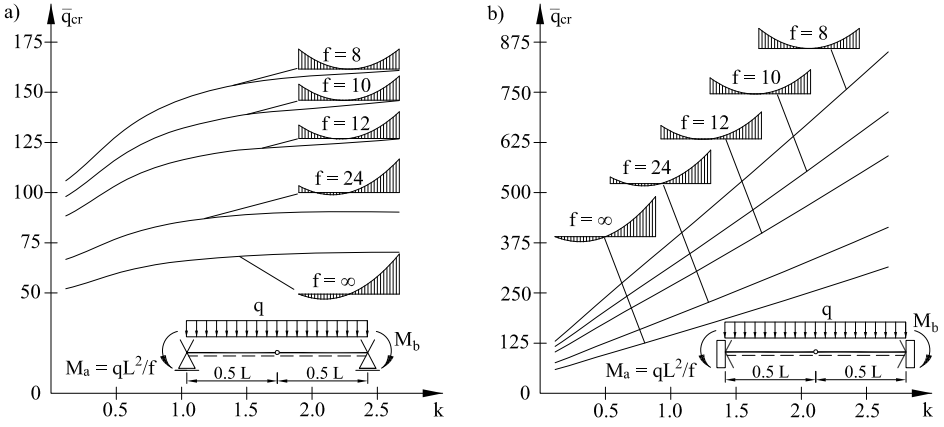

Figure 8: Critical loads for beam with hinge at α = 0.5

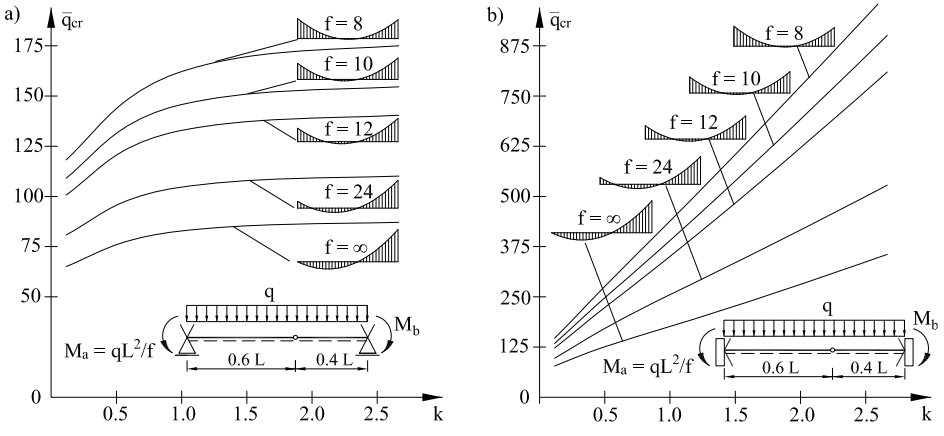

Figure 9: Critical loads for beam with hinge at α = 0.6

4 LATERAL TORSIONAL BUCKLING RESISTANCE

4.1 Lateral torsional buckling resistance according to Eurocode 3

The resistance according to EC3 [2, 6.3.2.3] for hot rolled sections is

$$M_{R,d}^{EC3} = \chi_{LT} \frac{M_{pl,y}}{\gamma_{M1}} = \left(\frac{1}{\Phi_{LT} + \sqrt{\Phi_{LT}^2 - \beta \bar{\lambda}_{LT}^2}} \right) \frac{M_{pl,y}}{\gamma_{M1}} \quad \begin{cases} \leq 1{,}0 \\ \leq \dfrac{1}{\bar{\lambda}_{LT}^2} \end{cases} \qquad \Phi_{LT} = 0{,}5\left[1 + \alpha_{LT}\left(\bar{\lambda}_{LT} - \bar{\lambda}_{LT,0} \right) + \beta \bar{\lambda}_{LT}^2 \right] \quad (8)$$

The following investigation was carried out for beams with variable span L, moment hinges and IPE300 section (section class 1 [2, table 5.2], buckling curve b [2, table 6.4] and imperfection coefficient $\alpha_{LT} = 0{,}34$ [2, table 6.4]). Further it is conservatively assumed that $\beta = 0{,}75$, $\gamma_{M1} = 1{,}1$, $\bar{\lambda}_{LT,0} = 0{,}4$ and $f = 1$. For lateral buckling capacities with $\alpha = 0.5$ (fig. 10a) $M_a = M_a = qL^2/8$ and for $\alpha = 0.4$ (fig. 10b) and $M_a = qL^2/12$ the moment $M_b = 0.175qL^2$. Again boundary conditions at both ends are such that rotations about z-axis are restrained and warping unconstrained.

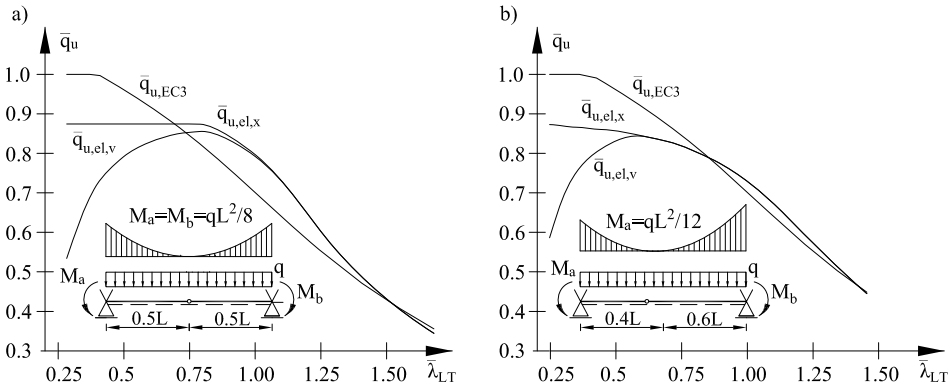

Figure 10: Dimensionless lateral torsional buckling resistance

Figures 10a and 10b show dimensionless load capacities depending on the dimensionless buckling slenderness $\bar{\lambda}_{LT}$. Curves $\bar{q}_{u,EC3}$ in fig. 10 are obtained by dividing the ultimate load derived from eqn. (8) by the load q_{pl} associated with fully plastic moment. They agree with the χ_{LT}-distribution. It is to notice that eqn. (8) does not take into account the effect of shear forces. Therefore the cross section resistance has to be checked additionally and will restrict the capacity - specifically for small buckling slendernesses - with respect to provisions in [2, 6.2.8].

4.2 Lateral torsional buckling resistance based on theory 2nd order analysis

Figure 11: Lateral torsional buckling mode of tapered beam with moment hinge

For stability design of more general structures like continuous beams with discrete or continuous elastic support, arbitrary boundary conditions, intentionally out-of-plane loading and variable cross section (see fig. 11) a theory 2nd order three-dimensional stress analysis with geometric out-of-plane imperfections leads to a generally applicable approach.

For class 1 cross sections two criterions [5], [6] are available for definition of the ultimate load capacity

- theory 2nd order first yield criterion
- theory 2nd order first hinge criterion

For first yield design the von-Mises stress σ_v anywhere along the beam axis within the cross section, obtained from a theory second order analysis of the geometrically imperfect structure with linear elastic material behaviour must satisfy

$$max\,\sigma_V^{II} = \sqrt{(\sigma_{x,d}^{II})^2 + 3(\tau_d^{II})^2} \le \frac{f_y}{\gamma_{M0}} \tag{9}$$

In (9) $\sigma_{x,d}^{II}$ is the theory 2nd order axial stress due to the combined action an axial force N, bending moments M_y and M_z about principal axis and the warping moment M_ω from nonuniform torsion. The theory 2nd order shear stress τ_d^{II} is calculated from shear forces V_y and V_z and the St. Venant's torsion moment M_{TP}. Graphs $\bar{q}_{u,el,v}$ in figs. 10 are obtained by dividing the ultimate load derived from eqn. (9) by the q_{pl}. From comparison with the $\bar{q}_{u,el,x}$ curve, which neglects shear stresses in eqn. (9) it is obvious, that in the stocky slenderness area the capacity is essentially limited by the shear stresses. In the moderate slender area the first yield criterion leads, depending on the moment distribution, to somewhat higher capacities than the equivalent slenderness approach of EC3. For very slender structures shear stresses do not count and capacities are very similar.

5 CONCLUSION

A procedure has been developed for lateral torsional buckling design of continuous beams with moment hinges. It has been alternatively applied for equivalent slenderness procedure in EC3 and for first yield criterion on the basis of a geometrically nonlinear theory 2nd order stress analysis including geometric imperfections.

REFERENCES

[1] BTII-Programm, Biegetorsionstheorie II.Ordnung, *Friedrich + Lochner GmbH - Software für Statik und Tragwerksplanung, Version 03/09, Stuttgart/Dresden.*

[2] DIN EN 1993-1-1, Eurocode 3: Bemessung und Konstruktion von Stahlbauten, Teil 1-1: Allgemeine Bemessungsregeln und Regeln für den Hochbau, 2005.

[3] Trahair, N.S., Flexural-Torsional Buckling of Structures, *CRC Press Boca Ration, 1993, ISBN 0849377633.*

[4] Lindner, J., Stabilisierung von Trägern durch Trapezbleche, *Stahlbau 1/1987, Ernst & Sohn*

[5] Osterrieder, P., Voigt, M., Saal, H., Vergleichende Betrachtungen zum Biegedrillknicknachweis nach DIN 18800 Teil 2 (Ausgabe März 1988), *Stahlbau 58 (1989), Heft 11, 341 – 347*

[6] Osterrieder, P., Kretzschmar, J., First-hinge analysis for lateral buckling design of open thin-walled steel members, *Journal of Constructional Steel Research 62 (2006), pp. 35-43*